

## Variation of $f$ -electron localization in diluted US and UTe

J. Schoenes

*Institut für Halbleiterphysik und Optik, Technische Universität Braunschweig, D-38106 Braunschweig, Germany*

O. Vogt, J. Löhle, F. Hulliger, and K. Mattenberger

*Laboratorium für Festkörperphysik, Eidgenössische Technische Hochschule Zürich, CH-8093 Zürich, Switzerland*

(Received 25 October 1995; revised manuscript received 13 February 1996)

The temperature dependence of the magnetization, the electrical resistivity, and the Hall effect has been measured for 11 different uranium concentrations in single crystals of  $U_xLa_{1-x}S$  and is compared with corresponding data for  $U_{0.2}(La_{0.15}Y_{0.85})_{0.8}Te$  and UTe. While the electrical transport data for diluted UTe show maxima related to crystal-field splittings, such structures are absent in all sulfide compounds. The magnetic susceptibility of the sulfides, measured up to 1200 K, is fitted by the sum of a Curie-Weiss and a Pauli paramagnetism term in second-order approximation. In a quasi-free-electron model the variation with the uranium concentration of the Fermi energy, the carrier concentration and the effective mass is derived. It is found that the degree of localization varies nonmonotonically and, in a certain range, contrary to the U-U separation. It is concluded that hybridization and magnetic exchange play dominant roles. [S0163-1829(96)00921-6]

### I. INTRODUCTION

In general the degree of localization of  $5f$  electrons in the actinides lies between that of  $4f$  electrons in the lanthanides and that of  $3d$  electrons in transition-metal elements. Therefore, the study of  $5f$  systems is thought to allow to bridge the gap between localized and itinerant states.<sup>1</sup> Although many uranium compounds with a large variety of direct  $5f$ - $5f$  separation have been investigated, it appears that among the concentrated metallic uranium systems only UPd<sub>3</sub> is undoubtedly a localized  $5f$  system with a well-defined crystal-field splitting of the  $5f^2$  state resulting in a  $\Gamma_1$  and a  $\Gamma_{1a}$  ground state for the hexagonal and quasicubic sites, respectively.<sup>2</sup> A less clear situation is encountered in UTe. This material belongs to the class of ferromagnetic uranium monochalcogenides (see Table I), in which the Curie temperature decreases and the paramagnetic as well as the ordered magnetic moments increase with increasing lattice parameter, i.e.,  $5f$ - $5f$  separation. Nevertheless, the values of  $2.7\mu_B/U$  for the paramagnetic and  $2.25\mu_B/U$  for the ordered neutron moment of UTe are substantially smaller than the free-ion values for either the  $5f^2(^3H_4)$  configuration (3.58 and  $3.2\mu_B/U$ ) or the  $5f^3(^4I_{9/2})$  configuration (3.62 and  $3.27\mu_B/U$ ). Neutron scattering<sup>2</sup> shows magnetic excitations in the ferromagnetic phase, but no crystal-field level in the paramagnetic phase. The electrical resistivity<sup>3,4</sup> displays an itinerant behavior in US and a Kondo-type behavior in the paramagnetic phase of UTe. The elastic constants<sup>5</sup> of UTe are anomalous with a negative  $c_{12}$ , as is typical for intermediate valent lanthanide monochalcogenides.<sup>6</sup>

Because tellurium is the largest chalcogen for which the growth of macroscopic uranium monochalcogenide single crystals is possible (the next element in the column is the very rare, short-living radioactive polonium), the only way to increase further the  $5f$ - $5f$  separation in this class of compounds is the dilution with nonmagnetic elements. First attempts to dilute UTe with LaTe (Ref. 7) showed a phase

separation when more than 20 at. % of uranium were substituted by La. Recently, some of us succeeded in growing single crystals in which 80 at. % of uranium have been substituted by a combination of 15 at. % La and 85 at. % Y.<sup>8</sup> In a brief letter<sup>9</sup> we reported that electrical transport and susceptibility measurements for these crystals showed clear evidence for crystal-field splitting. If one attributes this appearance of crystal-field levels in diluted UTe to a pure  $5f$ - $5f$  separation effect, as has been proposed in the past and as is suggested from the behavior within the series of the concentrated uranium monochalcogenides, other very diluted uranium monochalcogenides should show similar signs of increasing localization with increasing dilution. In this paper we report on a systematic study of the effect of diluting US with LaS, a pseudobinary compound system which is free of the metallurgical problems encountered in the dilution of UTe. Single crystals of  $U_xLa_{1-x}S$  with  $x$  varying from 0 to 1 can be grown with sizes of several mm<sup>3</sup>. X-ray diffraction and the microscopic analysis of polished and etched surfaces show no indications of a second phase. Magnetic susceptibility and electrical resistivity measurements up to 1200 K and Hall-effect data up to 300 K in fields up to 10 T show that diluted US behaves very differently from diluted UTe. There is no evidence for crystal-field splitting, even not for a sample containing only 8 at. % U. Instead, we find a substantial temperature-dependent Pauli susceptibility. A quantitative analysis of the data leads to a nonmonotonic uranium-concentration-dependent effective mass for a strongly hybridized  $f$ - $d$  conduction band. It is suggested that in this system magnetic exchange enhances localization.

### II. EXPERIMENTAL DETAILS

Single crystals of  $U_xLa_{1-x}S$  with  $x = 0, 0.08, 0.15, 0.30, 0.40, 0.50, 0.55, 0.60, 0.80, 0.90,$  and  $1.00$  have been prepared by the mineralization method described in detail elsewhere.<sup>10</sup> In addition  $U_{0.2}(La_{0.15}Y_{0.85})_{0.8}Te$  and UTe crys-

TABLE I. Some physical properties of the uranium monochalcogenides suggesting increasing localization with increasing lattice parameter (after /2/).

	Lattice parameter (Å)	Curie temperature (K)	Paramagnetic moment ( $\mu_B/U$ )	Ordered moment ( $\mu_B/U$ ) (neutron)
US	5.489	180	2.25	1.7
USe	5.744	160	2.5	2.0
UTe	6.155	104	2.7	2.25

tals have been grown by the same method. The magnetization has been measured between 2 and 300 K in fields up to 10 T with a computer-controlled moving sample magnetometer. Magnetic measurements from 300 to 1200 K have been performed with a Faraday balance in external fields up to 0.5 T. Typical sample volumes were 10 mm<sup>3</sup>. The contribution of the sample holder was carefully determined and subtracted from the high-temperature magnetic susceptibility measurements. Data collected with the same equipment and method on YbP showed perfect Curie-Weiss behavior over the whole temperature range, indicating that the deviations to be reported here for diluted US and UTe are intrinsic and not an artifact of the contribution from the sample holder.

All electrical transport measurements have been done with the van der Pauw method.<sup>11</sup> The samples were shaped in the form of thin platelets with typical dimensions of 3×3×0.5 mm. Resistivity and Hall-effect data were collected between 2 and 300 K with magnetic fields up to 10 T. The contacts consisted of spring-loaded tungsten tips pressed in a square arrangement near the edges of a (100) surface of the crystals. During the measurements the samples were immersed in the helium gas stream of a variable-temperature cryostat. For measuring the electrical resistivity between 300 and 1000 K we have developed a special setup in order to prevent oxidation of the samples and deterioration of the contacts.<sup>12</sup> The sample in form of a square thin platelet is squeezed between four tungsten wires coming out of a ceramic (Al<sub>2</sub>O<sub>3</sub>) tube with four holes. The tungsten wires are electrochemically thinned at the location of the sample and the distance between the end of the ceramic tube and the sample determines the contact pressure. At the opposite end of the approximately 10 cm long ceramic tube, the tungsten wires are fed through the top of a quartz tube. After mounting the sample, the quartz tube is sealed under a low pressure of helium gas (at room temperature). Fresh cerium turnings at the bottom of the quartz tube getter any remaining oxygen or water and ensure that the samples do not deteriorate by oxidation. Variable temperatures are achieved by putting the quartz tube in a temperature-stabilized oven and allowing sufficient time for the system to reach a given temperature.

### III. EXPERIMENTAL RESULTS

The temperature dependence of the inverse susceptibility is depicted in Fig. 1 for a selected number of uranium concentrations. All curves (right ordinates) deviate strongly from the linear Curie-Weiss behavior. Because, as we will see later, neither the resistivity nor the Hall effect display

TABLE II. Lattice parameter and parameters derived from a fit of the inverse magnetic susceptibility of U<sub>x</sub>La<sub>1-x</sub>S with Eq. (1). The inclusion of a Pauli paramagnetism term in second approximation for US improves considerably the fit at higher temperatures. This is the reason for the difference in  $\mu_{\text{eff}}$  between Tables I and II.

U <sub>x</sub> La <sub>1-x</sub> S	$a$ (Å)	$\theta_p$ (K)	$\mu_{\text{eff}}$ ( $\mu_B/U$ )	$\chi_0$ [ $10^{-6}$ emu/mol U]	$c$ ( $10^{-8}$ K <sup>-2</sup> )
$x$					
0.08	5.834	-52	2.35	900	9
0.15	5.808	-20	2.21	1000	9
0.30	5.751	0	2.23	900	9
0.40	5.713	71	2.31	470	9
0.50	5.674	56	2.16	490	9
0.55	5.655	86	2.06	500	9
0.60	5.636	91	2.47	300	9
0.80	5.560	142	2.30	310	9
0.90	5.522	177	2.24	310	9
1.00	5.484	184	2.38	370	9

structures which would indicate some excited level in this temperature range, we do not make a van Vleck ansatz as for U<sub>0.2</sub>(La<sub>0.15</sub>Y<sub>0.85</sub>)<sub>0.8</sub>Te,<sup>9</sup> but will fit the data by adding a Pauli paramagnetism term to the Curie-Weiss term. However, contrary to previous, so-called modified Curie-Weiss fits,<sup>13</sup> which took into account only the leading temperature-independent term of the Pauli paramagnetism expression, we found that excellent fits up to 1200 K require the inclusion of the second, temperature-dependent term arising from the Sommerfeld expansion of the chemical potential. This need to consider the expansion of the chemical potential as function of the Fermi energy (at  $T=0$  K) follows already from the large values of the Pauli susceptibility. Indeed, Pauli susceptibility values of several hundred times  $10^{-6}$  emu/mol are one order of magnitude larger than that for a conventional metal like sodium, indicating Fermi temperatures of only a few thousand K. Thus for the susceptibility fits we use the expression<sup>14</sup>

$$\chi = \frac{C}{T - \theta_p} + \chi_0 \left\{ 1 - \frac{\pi^2}{12} \left( \frac{k_B T}{E_F} \right)^2 \right\}. \quad (1)$$

Here  $C$  is the Curie constant,  $\theta_p$  is the paramagnetic Curie temperature, and  $E_F$  is the Fermi energy. Figure 1 shows these fits plotted as  $(\chi_{\text{meas}} - \chi_{\text{Pauli}})^{-1}$  versus the temperature  $T$ , where  $\chi_{\text{Pauli}} = \chi_0(1 - cT^2)$ . Table II displays the fit parameters for all investigated U<sub>x</sub>La<sub>1-x</sub>S compounds. The most stringent result is that the constant  $c$  is independent of the uranium concentration which implies that the Fermi energies of all investigated diluted uranium sulfide compounds are identical and equal to 0.26 eV. Figure 2 gives, as an example, for the sample with  $x=0.15$  an impression of the sensitivity of the fits. As can be seen, a fit without the inclusion of the temperature-dependent term is unsatisfactory for temperatures exceeding 600 K. The fit with a constant  $c$  twice as large as ideal, i.e., a Fermi energy reduced by a factor  $\sqrt{2}$ , deviates already for  $T > 300$  K. Pure LaS shows a much weaker deviation from a temperature-independent Pauli susceptibility and, within the accuracy of our measurements, the fit of the inverse susceptibility does not require

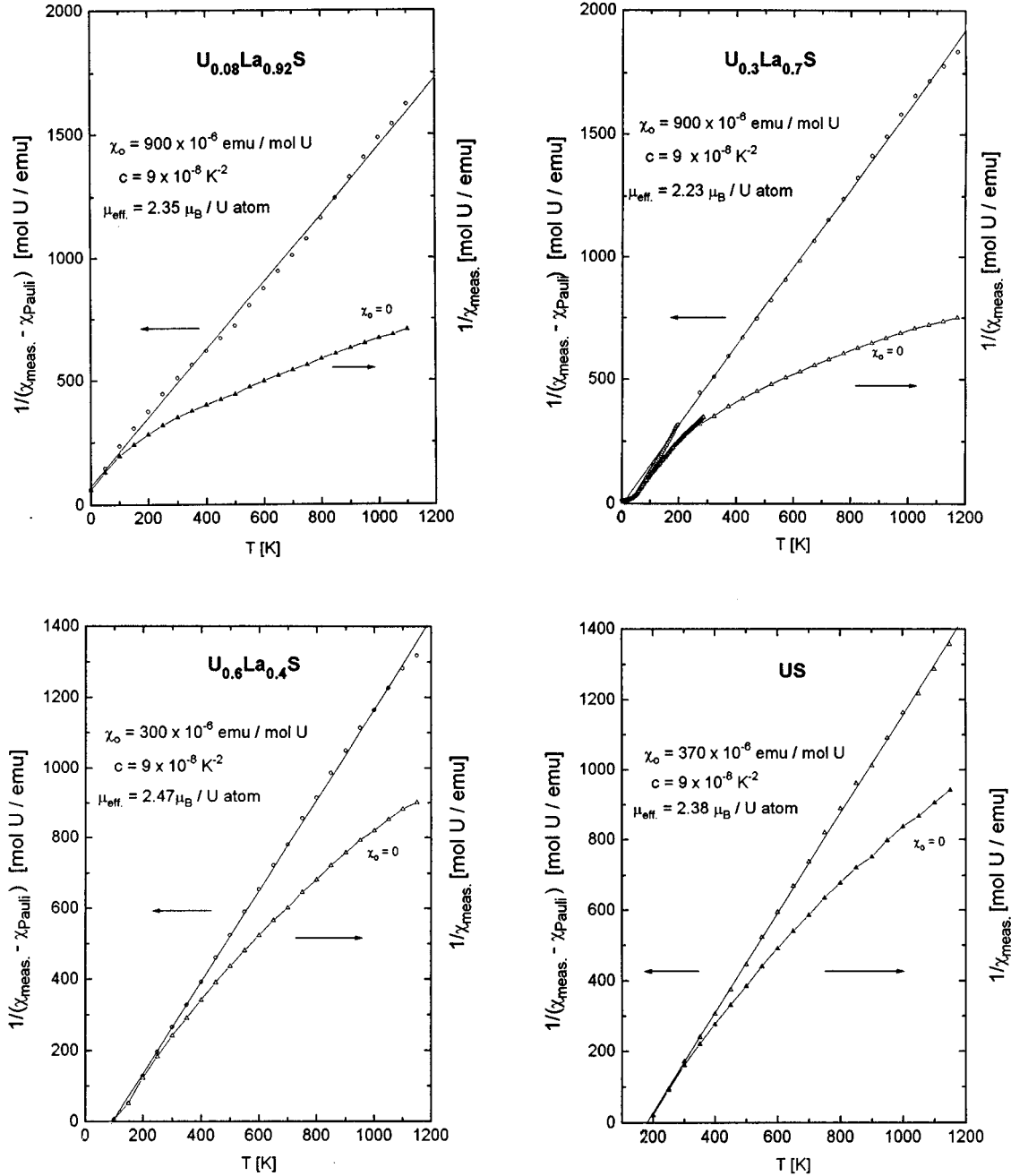


FIG. 1. Temperature dependence of the inverse susceptibility (right ordinate) and fit with Eq. (1) (left ordinate) of  $U_xLa_{1-x}S$  for  $x=0.08$ ,  $0.30$ ,  $0.60$ , and  $1.00$ . For the fits with Eq. (1) the parameters for the Pauli susceptibility,  $\chi_0$  and  $c$ , have been varied so that  $(\chi_{\text{meas}} - \chi_{\text{Pauli}})^{-1}$  comes as close as possible to a straight line.

the inclusion of the temperature-dependent term. A monotonic increase of the paramagnetic Curie temperature  $\theta_p$  with the uranium concentration  $x$  is found for  $x$  between  $0.08$  and  $1$  (Fig. 3). The negative values for  $x$  below the percolation limit of  $0.15$  indicate an antiferromagnetic coupling in the highly diluted limit when exchange forces between ions become small. Magnetization measurements at high magnetic fields and low temperatures reveal an interesting transition between the moments at low and high uranium concentrations. As depicted in Fig. 4 a rather sudden increase of the moment from about  $0.3\mu_B/\text{U atom}$  at low  $U$  concentration to an anisotropic moment ranging from  $0.9$  to  $1.55\mu_B/\text{U atom}$  for  $US$  occurs near  $x=0.5$ . Actually, the increase starts at

$x=0.3$  where ferromagnetic order sets in and the moments become nearly concentration-independent above  $x=0.8$ . A last parameter obtained from the fits is the Pauli susceptibility constant  $\chi_0$ . Its dependence on the uranium concentration is, as we will discuss in Sec. IV, somewhat more complex. Roughly speaking, its trend is opposite to that of the magnetic moment at low temperatures and high fields. The magnetic susceptibility of  $LaS$  has been determined to be  $40 \times 10^{-6} \text{ emu/mol}$  or  $1.33 \times 10^{-6} \text{ emu/cm}^3$ .

The temperature dependence of the inverse magnetic susceptibility of  $U_{0.2}(La_{0.15}Y_{0.85})_{0.8}Te$  deviates much less from a straight line. Instead a very weak and broad bump appears between  $50$  and  $250$  K. Figure 5 shows the data up to  $400$  K

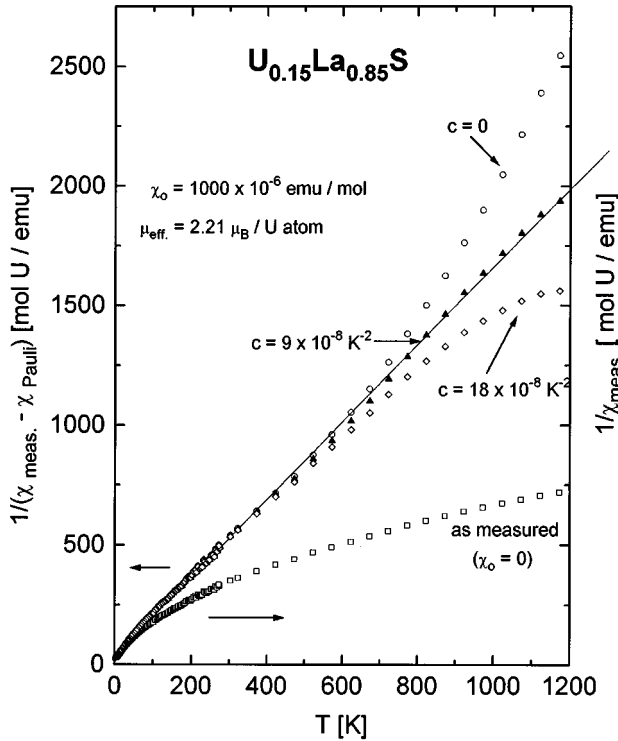


FIG. 2. Demonstration of the sensitivity of the fits with Eq. (1) of the temperature dependence of the inverse susceptibility for  $U_{0.15}La_{0.85}S$ .

and a fit with a van Vleck expression for an  $f^3$  configuration split by the crystalline electric field.<sup>9</sup> This fit with a van Vleck term gets its main justification from the existence of both a maximum in the resistivity and in the Hall effect near 50 K. In an octahedral crystal-electric field the  $f^3$  free-ion state splits into the states  $\Gamma_8^{(1)}$ ,  $\Gamma_8^{(2)}$ , and  $\Gamma_6$ , with  $\Gamma_8^{(1)}$  likely being the ground state.<sup>15</sup> Assuming then that  $\Gamma_8^{(2)}$  is the first excited state, one derives from the general expression given for example by Schieber<sup>16</sup>

$$\chi_{\nu V} = \frac{N\mu_B^2 g^2}{4 + 4e^{-\Delta_1/k_B T} + 2e^{-\Delta_2/k_B T}} \left\{ \left[ \frac{|\langle \Gamma_8^{(1)} | J_z | \Gamma_8^{(1)} \rangle|^2}{k_B T} + 2 \frac{|\langle \Gamma_8^{(1)} | J_z | \Gamma_8^{(2)} \rangle|^2}{\Delta_1} + 2 \frac{|\langle \Gamma_8^{(1)} | J_z | \Gamma_6 \rangle|^2}{\Delta_2} \right] + \left[ \frac{|\langle \Gamma_8^{(2)} | J_z | \Gamma_8^{(2)} \rangle|^2}{k_B T} - 2 \frac{|\langle \Gamma_8^{(2)} | J_z | \Gamma_8^{(1)} \rangle|^2}{\Delta_1} + 2 \frac{|\langle \Gamma_8^{(2)} | J_z | \Gamma_6 \rangle|^2}{\Delta_{21}} \right] e^{-\Delta_1/k_B T} + \left[ \frac{|\langle \Gamma_6 | J_z | \Gamma_6 \rangle|^2}{k_B T} - 2 \frac{|\langle \Gamma_6 | J_z | \Gamma_8^{(1)} \rangle|^2}{\Delta_2} - 2 \frac{|\langle \Gamma_6 | J_z | \Gamma_8^{(2)} \rangle|^2}{\Delta_{21}} \right] e^{-\Delta_2/k_B T} \right\}. \quad (2)$$

Here  $\Delta_1$  is the energy difference between  $\Gamma_8^{(2)}$  and  $\Gamma_8^{(1)}$ ,  $\Delta_2$  is the energy difference between  $\Gamma_6$  and  $\Gamma_8^{(1)}$  and  $\Delta_{21}$  is the energy difference between  $\Gamma_6$  and  $\Gamma_8^{(2)}$ . The matrix elements have been calculated using the wave functions of Lea, Leask, and Wolf<sup>17</sup> and the value 1 for the parameter which repre-

sents the ratio of the crystal-field parameters of sixth and fourth order as proposed by Hu and Cooper.<sup>15</sup> The values for these matrix elements squared are in the order of appearance in Eq. (2) 24.244, 7.922, 0.833, 16.133, 7.922, 8.944, 6.724, 0.833, and 8.944. Because of the reduction of the paramagnetic moment compared to the free-ion value, Eq. (2) has been divided by a reduction factor  $F=1.55$ . The best fit, shown in Fig. 5, is obtained with the level separations  $\delta_1 = \Delta_1/k_B = 50$  K and  $\delta_2 = \Delta_2/k_B = 400$  K. The fit of the magnetic susceptibility is moderately sensitive to  $\delta_1$  and very insensitive to  $\delta_2$ . Thus, it is hard to distinguish between  $\delta_1 = 50$  and 70 K, but 100 K gives clearly a worse fit. No significance should be given to the value of  $\delta_2$ .

An overview of the temperature dependence of the electrical resistivity, in zero magnetic field of the pseudobinary  $U_xLa_{1-x}S$  solid solutions is shown in Fig. 6. One observes transitions from a pure electron-phonon-type resistivity with a positive temperature coefficient in LaS to a Kondo-type behavior with a negative temperature coefficient at lower temperatures for  $x \leq 0.5$  to a ferromagnetic-order dominated behavior with a strong positive temperature coefficient at low temperatures and a much weaker positive gradient at  $T > T_C$  for  $x \geq 0.8$ . A special case is the sample with  $x = 0.6$ . It combines features of strong ferromagnetic order at lower temperatures and a Kondo-type decrease of the resistivity at high temperatures. Its resistivity curve is very reminiscent of that for pure UTe.<sup>4</sup>

Figure 7 shows the resistivity for the two lower uranium concentrations in more detail. We see the increase of the logarithmic Kondo contribution with increasing  $x$ . Although quantitative fits with the expression<sup>18</sup>

$$\rho(T) = \rho_0 + \rho_m + c_K \ln \frac{k_B}{0.77D} + c_{ph} T - T_{min} c_{ph} \ln T \quad (3)$$

are not perfect as becomes clear comparing the full line with the experimental points for  $U_{0.15}La_{0.85}S$ , there is no indication of magnetic scattering on two or more crystal-field split levels, like for example in the cerium monochalcogenides.<sup>19</sup> This is also in strong contrast to the resistivity of the diluted uranium telluride analog  $U_{0.2}(La_{0.15}Y_{0.85})_{0.8}Te$ , displayed in Fig. 8, which shows a maximum of the resistivity at 50 K and a Kondo-like behavior at higher temperatures.

The Hall-effect measurements support these conclusions. Figure 9 presents an overview of the Hall data for eight different concentrations and Fig. 10 provides details for the two lower uranium concentrations. For  $x = 0.08$  the Hall coefficient is dominantly negative. It is only below 100 K that the extraordinary Hall contribution, which is proportional to the magnetization, becomes visible. This extraordinary Hall effect is positive, while the ordinary Hall effect is negative. With a doubling of the uranium concentration the extraordinary Hall contribution dominates the ordinary Hall effect at temperatures below 120 K. For all samples studied with higher uranium concentrations the extraordinary part of the Hall effect dominates over the full temperature range from 2 to 300 K, leading to a positive total Hall effect. Furthermore, the magnetic order of these samples manifests itself by the appearance of a maximum shifting to higher temperature with increasing uranium concentration. In contrast to the discussed absence of a peak in the temperature dependence of the Hall coefficient for very diluted pseudobinary uranium

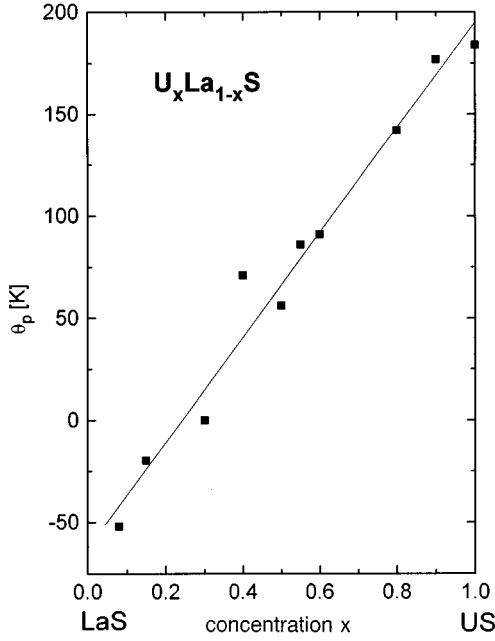


FIG. 3. The concentration dependence of the paramagnetic Curie temperature of  $U_xLa_{1-x}S$  as derived from fits of the type displayed in Fig. 1.

sulfide solid solutions,  $U_{0.2}(La_{0.15}Y_{0.85})_{0.8}Te$  displays a pronounced peak near 30 K (Fig. 11). If one decomposes this total Hall effect into normal and extraordinary contributions using the empirical expression

$$R_H(T) = R_0 + 4\pi R_s \chi(T), \quad (4)$$

$R_s$  versus  $T$  is a horizontal straight line for  $50 < T < 300$  K and decreases strongly below 50 K.<sup>9</sup> Thus, the extraordinary,

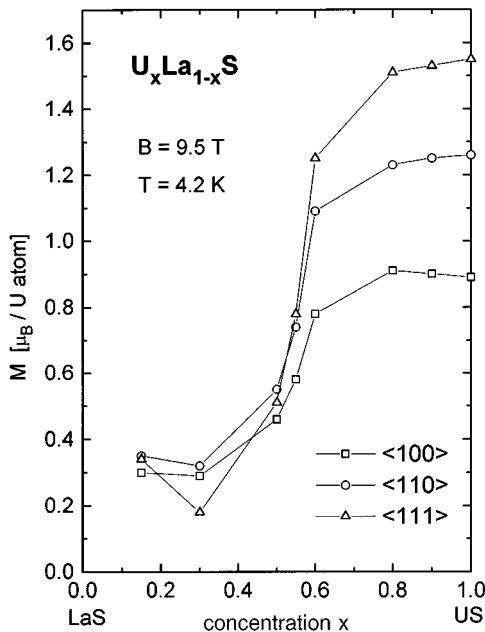


FIG. 4. The magnetization per uranium atom of  $U_xLa_{1-x}S$  at 2 K and 9.5 T as a function of  $x$  for different crystallographic orientations.

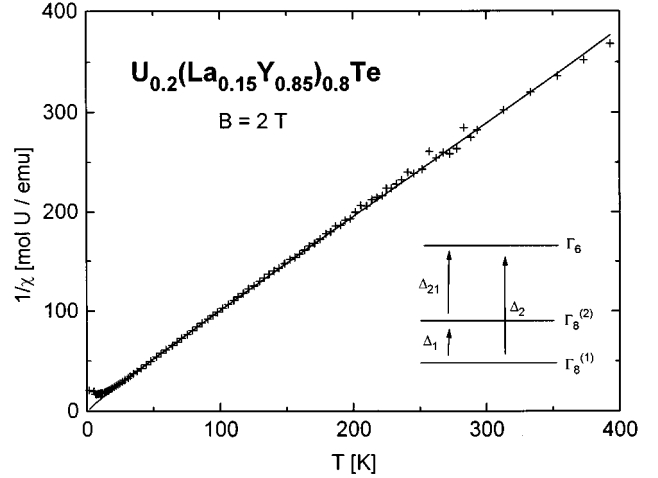


FIG. 5. Temperature dependence of the inverse susceptibility of  $U_{0.2}(La_{0.15}Y_{0.85})_{0.8}Te$  and fit with a van Vleck expression for a crystal-field split  $5f^3(^4I_{9/2})$  state (full line).

i.e., magnetic part of the Hall effect of  $U_{0.2}(La_{0.15}Y_{0.85})_{0.8}Te$  shows, like the magnetic susceptibility and the electrical resistivity, a structure at 50 K which we attribute to the crystal-field splitting of the  $5f^3$  state in this compound.

The application of Eq. (4) to the decomposition of the total Hall effect of the two sulfide samples with low uranium concentration is shown in Fig. 12. In a one-band model the values derived for  $R_0$  correspond to free-electron concentrations of 1.25 and 0.6 per formula unit for  $x=0.08$  and 0.15, respectively.

#### IV. DISCUSSION

Our experimental data reveal a substantial difference in the physical behaviors of magnetically diluted US and diluted UTe. While all data for  $U_{0.2}(La_{0.15}Y_{0.85})_{0.8}Te$  indicate that the  $5f$  electrons are localized, the situation in diluted US is much more complex. In the following we try to draw more quantitative conclusions from the experimental data. To do so, we assume the validity of the quasi-free-electron model.

For pure LaS we found a temperature independent susceptibility. For  $g=2$  and  $s=1/2$  the Pauli susceptibility  $\chi_{\text{Pauli}}(0) = \chi_0$  [in Eq. (1)] is related to the density of states at the Fermi energy  $D(E_F) = 3N/2E_F$  by

$$\chi_0 = \mu_B^2 D(E_F). \quad (5)$$

The Fermi energy can therefore be calculated from the Pauli susceptibility and the carrier concentration  $N$  using the relation

$$E_F = \frac{3}{2} \frac{\mu_B^2}{\chi_0} N. \quad (6)$$

For the carrier concentration  $N$  we assume 1 electron per formula unit ( $e/f.u.$ ) as suggested by the chemical formula. The measured temperature-independent susceptibility is the sum of the diamagnetic susceptibility of the core and the conduction electrons and the paramagnetic Pauli susceptibility of the conduction electrons. In the free-electron model  $\chi_0 = -3\chi_{\text{dia}}$ . However, in the quasi-free-electron model with

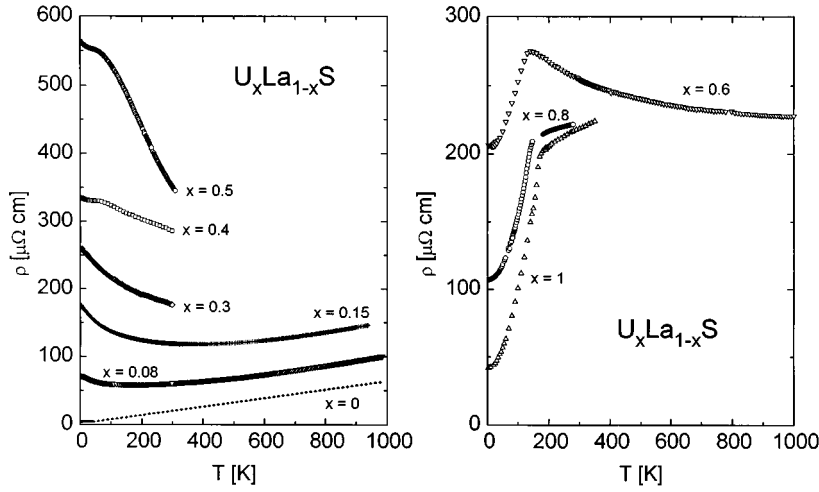


FIG. 6. Temperature dependence of the electrical resistivity of  $U_xLa_{1-x}S$  for various  $x$ .

an effective mass  $m^* > m$  the paramagnetic part is enhanced, while the diamagnetic contribution decreases approximately like  $m/m^*$ . Using together with Eq. (6) the expression for the effective mass

$$m^* = \frac{\hbar^2}{2E_F} (3\pi^2 N)^{2/3}, \quad (7)$$

and neglecting the diamagnetic susceptibility of the core, one derives by iteration  $m^* = 2.57 m$  and  $E_F = 1.05$  eV.

For all investigated sulfide compounds containing uranium the effective mass is substantially larger than the free-electron mass and the diamagnetic Landau susceptibility is negligible compared to the measured paramagnetic susceptibility. From the temperature-dependent Pauli term  $c$  defined in conjunction with Eq. (1) we obtain for the Fermi energy

$$E_F = \frac{\pi k_B}{\sqrt{12c}} \quad (8)$$

a value of 0.26 eV for all uranium-containing sulfides. Thus, hybridization of  $5f$  and  $d$  electrons leads to an effective conduction band which is substantially narrower than the  $5d$  band in pure LaS.

From the Fermi energy and the Pauli susceptibility, we can now compute the carrier density in this hybridized conduction band using the relations

$$N = \frac{2}{3} D(E_F) E_F = \frac{2}{3} \frac{\chi_0}{\mu_B^2} E_F. \quad (9)$$

The carrier density  $N$  and the Fermi energy  $E_F$  allow the calculation of the effective mass in the quasi-free-electron model using again Eq. (7). Figure 13 shows data from this analysis. On the left ordinate the conduction carrier density per formula unit is given. The right ordinate displays the effective mass normalized to the free-electron mass. Because  $m^*$  is proportional to  $N^{2/3}$  and  $E_F$  is constant the two sets of data follow roughly the same trend. We find that both quan-

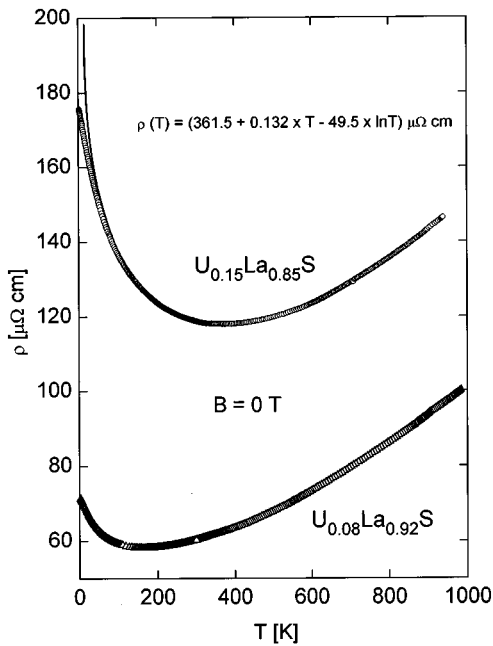


FIG. 7. Temperature dependence of the electrical resistivity of  $U_{0.08}La_{0.92}S$  and  $U_{0.15}La_{0.85}S$  and fit of the latter data with Eq. (3).

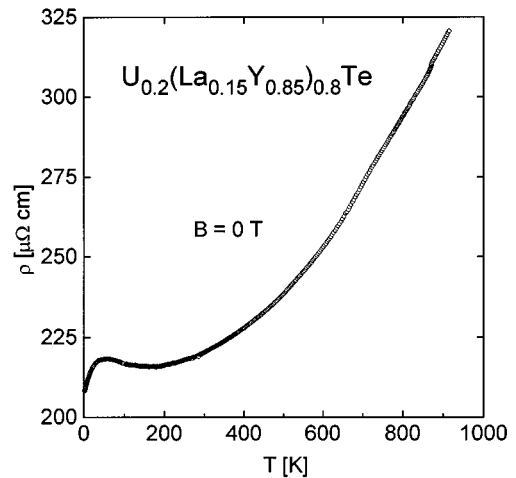


FIG. 8. Temperature dependence of the electrical resistivity of  $U_{0.2}(La_{0.15}Y_{0.85})_{0.8}Te$ .

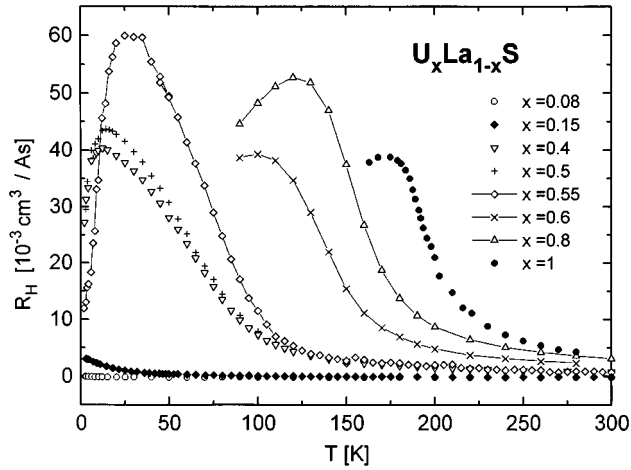


FIG. 9. Temperature dependence of the Hall coefficient of  $U_xLa_{1-x}S$  for various  $x$ .

ties show a remarkable nonmonotonic dependence on the uranium concentration. For diluted alloys up to  $x \sim 0.2$  the effective mass increases linearly with the uranium concentration from  $2.6 m$  to about  $11 m$ . At the same time the carrier density appears to go from 1 electron per formula unit through a minimum somewhere near  $x = 0.08$  to reach again approximately 1  $e/f.u.$  for  $x \sim 0.2$ . We think, however, that this result is an artifact of the models used for the reduction

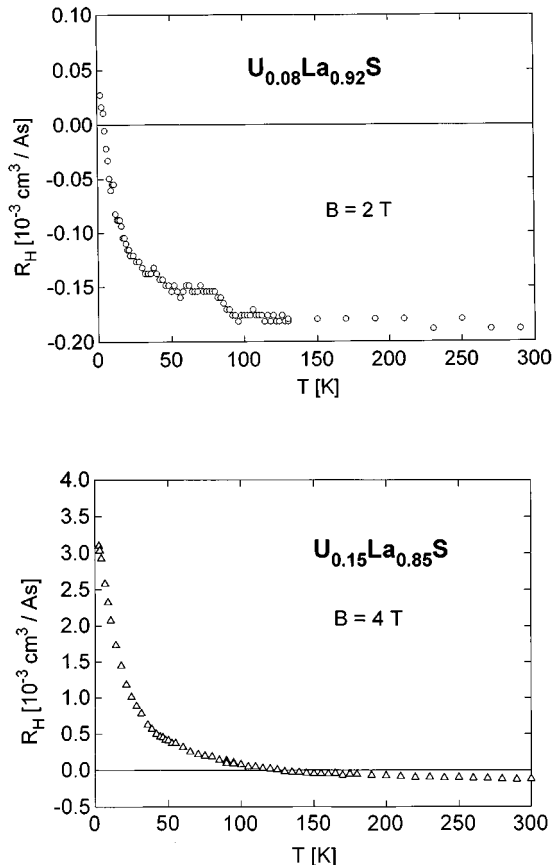


FIG. 10. Temperature dependence of the Hall coefficient of  $U_{0.08}La_{0.92}S$  and  $U_{0.15}La_{0.85}S$  in an applied field of 2 and 4 T, respectively.

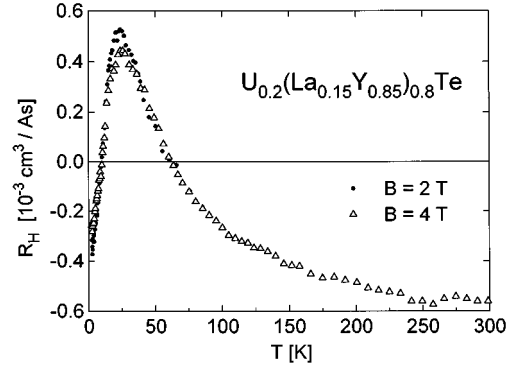


FIG. 11. Temperature dependence of the Hall coefficient of  $U_{0.2}(La_{0.15}Y_{0.85})_{0.8}Te$  in magnetic fields of 2 and 4 T.

of the data and, even more important, of the one-band model assumed in this discussion. First, the values for  $x = 0$  and  $x > 0$  are obtained from different models. Second, the constant Fermi energy for  $x > 0$  indicates that the temperature dependence of the Pauli susceptibility is governed by the  $f$  electrons, even for U concentrations as low as 0.08, when the contribution of  $d$  electrons to the density of states at the Fermi energy must still be substantial. If we replace Eq. (9) by a corresponding two-band equation and, consequently, split the value of  $72 \times 10^{-6}$  emu/mol for  $\chi_0$  into  $40 \times 10^{-6}$  emu/mol for the  $d$  electrons and  $32 \times 10^{-6}$  emu/mol for the  $f$  electrons and take Fermi energies of 1.05 and 0.26 eV for the  $d$  and  $f$  bands, respectively, we arrive at a carrier concentration  $N = 1.05 e/f.u.$  which comes quite close to the value of 1.25  $e/f.u.$  derived from the Hall-effect measurements. In a density of states scheme this two-band model can be represented as a horn near  $E_F$  of constant width, which grows out of the unhybridized conduction band in pure LaS. With increasing  $x$  the difference between the one-band and two-band model becomes smaller in respect to the derivation of the carrier concentration and strong hybridization between the  $f$  and  $d$  states calls for a description in terms of one hybridized conduction band.

If we compute the Pauli susceptibility per uranium atom  $\chi_{US}$  by making the ansatz

$$\chi_{U_xLa_{1-x}S} = \chi_{meas} = \chi_{LaS}(1-x) + \chi_{US}x, \quad (10)$$

the enhancement of the Pauli susceptibility per added uranium atom manifests itself in a huge increase of  $\chi_{US}$  for  $0 < x < 0.2$  (Fig. 14). Because the susceptibility contains also a Curie-Weiss term, not all  $f$  electrons need to participate in the hybridized conduction band. Assuming for the moment that the leveling-off near  $x = 0.3$  of  $N/N_0$  at a value of 1.3  $e/f.u.$  corresponds to an exhaustion of  $d$  electrons, then one of the three  $f$  electrons per uranium atom would contribute directly to the density of states at  $E_F$ , while the other two  $f$  electrons would sit in a split-off state below  $E_F$ .

For  $0.2 < x < 0.3$ ,  $m^*$  and  $N$  increase less rapidly and  $\chi_{US}$  goes through a maximum. For  $0.3 < x < 0.6$ ,  $m^*$  and  $N$  are nearly constant (Fig. 13) indicating that the  $f$  electrons added in this concentration regime do neither contribute directly to the density of states at  $E_F$  nor indirectly via polarization of other electrons. Consequently, the Pauli susceptibility per U atom (Fig. 14) decreases in this concentration range. It is the

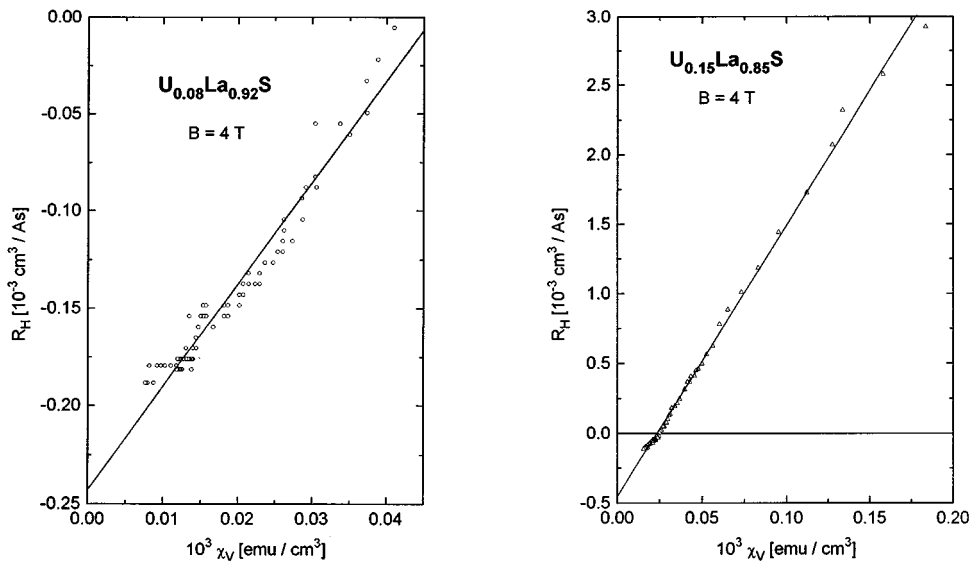


FIG. 12. Decomposition of the Hall coefficient of  $U_{0.08}La_{0.92}S$  and  $U_{0.15}La_{0.85}S$  into an ordinary and an extraordinary part following Eq. (4).

concentration range in which magnetic exchange becomes more and more dominant, the high-field moment increases from  $0.3$  to  $1.3\mu_B/U$  atom and the paramagnetic Curie temperature increases from  $0$  to  $90$  K (Table II). It is also the range in which the magnetic part of the electrical resistivity increases rapidly with  $x$  (Fig. 6). Thus, we can state that in this intermediate concentration range the added  $f$  electrons occupy the split-off state below the Fermi energy and form more or less local magnetic moments. The hybridized conduction electrons scatter on these increasing moments, explaining the large Kondo-type magnetic resistivity.

For  $x > 0.6$  or  $0.7$  the conduction carrier concentration and the effective mass increase again, while the Pauli susceptibility per uranium atom and the saturated magnetic moment are nearly constant. Obviously, an increase of the localiza-

tion of the split-off state much beyond the level reached for  $x = 0.6$  is not possible and the added  $5f$  electrons are distributed in both the hybridized  $fd$  conduction band and the split-off  $f$  state. The higher percentage of  $f$  character in the conduction band leads to an increase of the effective mass which in pure US is found to be about  $19m$ . The carrier concentration reaches  $2$  in US, indicating that the hybridized conduction band has the weight of one  $f$  and one  $d$  electron per uranium atom. The remaining  $f$  electron weight of  $2e/U$  goes into the more localized split-off state. Above  $x = 0.6$  or  $0.7$  the exchange has won the competition with the Kondo interaction. The Kondo-type resistivity with a negative temperature gradient disappears at the expenses of a typical ferromagnetic behavior with a positive gradient with  $\rho_{\text{magn}} \sim T^2$  for  $T < T_C$  and  $\rho \sim T$  for  $T > T_C$ .

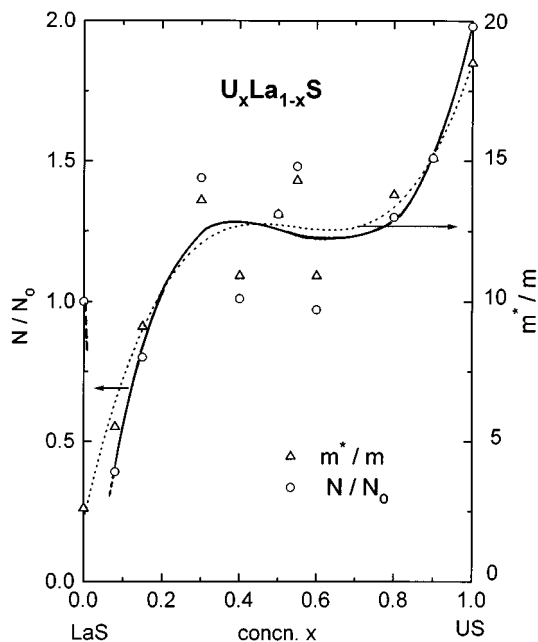


FIG. 13. Uranium-concentration dependence of the normalized number of conduction carriers and effective mass of these carriers in  $U_xLa_{1-x}S$ .  $N_0$  is the number of formula units per unit volume.

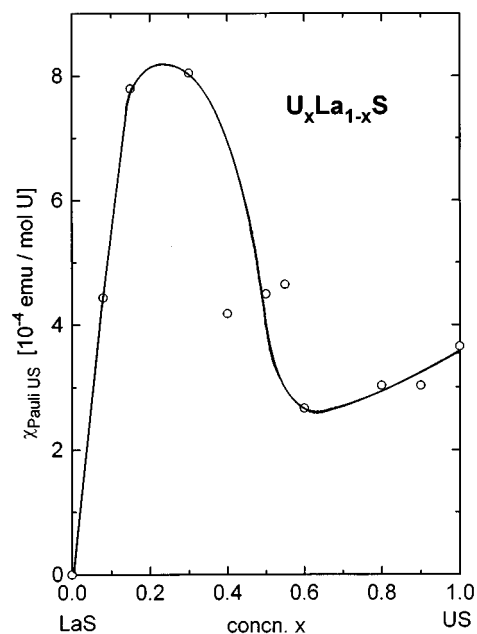


FIG. 14. Uranium-concentration dependence of the Pauli susceptibility per uranium atom in  $U_xLa_{1-x}S$ .



## V. CONCLUSION

We have shown from an analysis of magnetic and electrical data that magnetically diluted US behaves differently than diluted UTe. Thus, the models which relate localization simply with uranium-uranium separation can be incorrect, even for isostructural compounds. Hybridization of  $f$  electrons with  $d$  electrons from the cations and with  $p$  electrons from the anions play an often underestimated role. While strongly diluted UTe shows several signs of crystal-field splitting and pure UTe displays a Kondo-type temperature dependence of the electrical resistivity for  $T > T_C$ , even the strongest dilution of US does not lead to indications of crystal-field splitting, although the nearest U-U separation in  $U_{0.08}La_{0.92}S$  is given by the next-nearest cation separation of 5.8 Å. This exceeds largely the nearest U-U separation in  $U_{0.2}La_{0.15}U_{0.2}(La_{0.15}Y_{0.85})_{0.8}Te$  and UTe which are given by the nearest cation separation of 4.4 Å.

A detailed analysis of the experimental data of 11 sulfide samples with different uranium concentrations in the frame-

work of a quasi-free-electron model shows a nonmonotonic variation of the carrier concentration, the effective mass, and the degree of localization. We find three different regimes. For  $x < 0.1$  the system behaves according to the single-ion limit. Every added  $f$  electron contributes to an equal number of highly polarized conduction electrons. For  $0.3 < x < 0.6$  more and more relatively localized moments form under the action of magnetic exchange. In this regime it is evident that localization decreases with dilution, contrary to the naive expectation. For  $x > 0.7$  the "local" moments do not localize further, but the effective mass of the hybridized  $fd$  conduction band increases to reach nearly  $20 m$  for pure US.

## ACKNOWLEDGMENTS

The authors are indebted to P. Wachter for the support of this work. The technical assistance of P. Dekumbis is gratefully acknowledged. Part of this work has been financially supported by the Swiss National Science Foundation.

<sup>1</sup> *Handbook on the Physics and Chemistry of the Actinides*, edited by A. J. Freeman and G. Lander (North-Holland, Amsterdam, 1984), Vols. 1 and 2.

<sup>2</sup> W. J. L. Buyers and T. M. Holden, in *Handbook on the Physics and Chemistry of the Actinides* (Ref. 1), Vol 2, p. 239.

<sup>3</sup> J. Schoenes, B. Frick, and O. Vogt, *Phys. Rev. B* **30**, 6578 (1984).

<sup>4</sup> B. Frick, J. Schoenes, and O. Vogt, *J. Magn. Magn. Mater.* **47&48**, 549 (1985).

<sup>5</sup> J. Neuenschwander, H. Boppart, J. Schoenes, E. Voit, O. Vogt, and P. Wachter, in *Proceedings 14. Journées des Actinides, Davos 1984*, edited by J. Schoenes (ETH, Zürich, 1984), p. 30.

<sup>6</sup> P. Wachter, in *Handbook on the Physics and Chemistry of the Rare Earths*, edited by K. A. Gschneidner, Jr., L. Eyring, G. H. Lander, and G. R. Choppin (North-Holland, Amsterdam, 1994), Vol. 19, Chap. 132.

<sup>7</sup> J. Schoenes, B. Frick, and O. Vogt, *J. Appl. Phys.* **57**, 3149 (1985).

<sup>8</sup> O. Vogt and K. Mattenberger (unpublished).

<sup>9</sup> J. Schoenes, O. Vogt, and F. Hulliger, *J. Magn. Magn. Mater.* **140-144**, 1426 (1995).

<sup>10</sup> J. C. Spirlet and O. Vogt (Ref. 1), Vol. 1, p. 79.

<sup>11</sup> L. J. van der Pauw, *Philips Res. Rep.* **13**, 1 (1958).

<sup>12</sup> This method was developed by J. Schoenes and B. Frick and used in Ref. 4.

<sup>13</sup> J.-M. Fournier and R. Troc (Ref. 1), Vol. 2, p. 29.

<sup>14</sup> W. Nolting, *Quantentheorie des Magnetismus* (Teubner, Stuttgart, 1986), Vol. 1.

<sup>15</sup> G.-J. Hu and B. R. Cooper, *Phys. Rev. B* **48**, 12 743 (1993).

<sup>16</sup> M. M. Schieber, in *Selected Topics in Solid State Physics*, edited by E. P. Wohlfarth (North-Holland, Amsterdam, 1967).

<sup>17</sup> K. R. Lea, M. J. M. Leask, and W. P. Wolf, *J. Phys. Chem. Solids* **23**, 1381 (1962).

<sup>18</sup> B. Coqblin and J. R. Schrieffer, *Phys. Rev.* **185**, 847 (1969).

<sup>19</sup> J. Schoenes and F. Hulliger, *J. Magn. Magn. Mater.* **63&64**, 43 (1987).